

## Evaluation of Amyloid- $\beta$ Aggregation by Fourier Transform Infrared Spectrophotometer (FTIR)

Amyloid- $\beta$  is a peptide that consists of approximately 40 amino acid residues. Amyloid fibrils (fibrous aggregates), which occur as a result of the formation of parallel  $\beta$  sheets by intermolecular association of amyloid- $\beta$ , are the main component of the senile plaques (amyloid plaques) seen in the brains of Alzheimer's disease patients. Moreover, the formation mechanism and structure of amyloid fibrils have attracted great interest, as amyloid fibrils are also implicated in other neurodegenerative diseases, including Parkinson's disease<sup>(1)</sup>.

With FTIR, it is possible to evaluate the aggregation of amyloid- $\beta$  by analyzing the amide I band around  $1,650\text{ cm}^{-1}$ , which originates from stretching vibrations of the C=O group of the peptide bond. Fig. 1 shows the peptide bond structure. The secondary structures ( $\alpha$ -helix,  $\beta$ -sheet,  $\beta$ -turn, random coil, and other local 3-dimensional conformational features) of the amyloid- $\beta$  peptide can be obtained by curve fitting (peak splitting). Curve fitting is method in which the waveforms of each absorption band are expressed by an approximate curve such as a Lorentzian curve or Gaussian curve, and the peak information (position, intensity, full width at half maximum) of the approximate curve of each absorption band is optimized so as to minimize the difference between the calculated spectrum and the measured spectrum<sup>(2)</sup>. This article introduces the results of an evaluation of amyloid- $\beta$  aggregation.

R. Fuji, K. Maruyama, S. Iwasaki

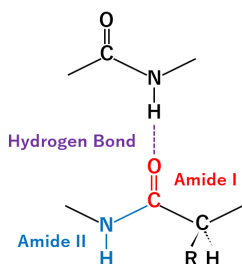


Fig. 1 Structural Diagram of Peptide Bonds

### ■ Instruments and Measurement Conditions

In these measurements, a Shimadzu IRTracer™-100 Fourier transform infrared spectrophotometer and a MicromATR™ attenuated total reflectance (ATR) measurement accessory (Czitek, LLC.) were used. The ATR method makes it possible to obtain a spectrum simply by placing the sample in close contact with the crystal, and cleaning after measurements is also simple in comparison with the transmission method. Moreover, the 9 reflection ATR crystal of the MicromATR accessory enables measurement with higher sensitivity than with the widely-used single reflection devices. Here, it may be noted that the optical system was purged with dry air because the peaks of the amide I band and water vapor overlap.

Table 1 Measurement Conditions

Instruments	: IRTracer-100
	: MicromATR™ (9 reflection ATR crystal)
Resolution	: $4\text{ cm}^{-1}$
Accumulation	: 100 times
Zero filling	: 4 ×
Apodization function	: Sqr-Triangle
Detector	: DLATGS

### ■ Experimental Procedure

Samples were prepared by dissolving amyloid- $\beta$  (human, 1-40) to approximately  $10\text{ }\mu\text{M}$  with ultrapure water, and ATR measurements were carried out after allowing the samples to stand at  $25\text{ }^\circ\text{C}$  for 0.5, 1, 2, 3, 24, 48, or 120 h. In this experiment,  $60\text{ }\mu\text{L}$  of the amyloid- $\beta$  solution was dripped ( $30\text{ }\mu\text{L} \times 2$  times) on the ATR crystal, the water content was completely removed with dry air, and the exsiccated amyloid- $\beta$  on the crystal was then measured.

Although the 9 reflection ATR crystal is intended for use exclusively with liquids, it is possible to measure samples in solid form after exsiccation of the liquid on the crystal as described above. After the measurement, the crystal was cleaned by wiping off the sample on the crystal with water without applying force.

### ■ Curve Fitting Procedure

The secondary structures of the amyloid- $\beta$  were identified by the following procedure.

- From 10 to 14 negative peaks were detected in the range of  $1,700\text{ cm}^{-1}$  to  $1,600\text{ cm}^{-1}$  in the second derivative spectrum of amyloid- $\beta$ . These peaks were used as the designated wavenumbers when conducting curve fitting.
- In this analysis, curve fitting was done by using the Lorentzian function. The conditions were adjusted to obtain the best match of the infrared spectrum of amyloid- $\beta$  before curve fitting and the synthesized spectrum of the peaks separated by curve fitting in the range of  $1,750\text{ cm}^{-1}$  to  $1,575\text{ cm}^{-1}$ .
- The secondary structure types were assigned to the separated peaks based on Reference<sup>(3)</sup>. The fraction of each type of secondary structure was calculated by the ratio to the total area of each curve.

### ■ Measurement Results

Fig. 2 shows the amide I band in the infrared spectrum of amyloid- $\beta$ . The spectra in Fig. 2 have been normalized so that the maximum peak intensity of the amide I band shows absorbance of 0.03. The peak at  $1,626\text{ cm}^{-1}$  (0.5 h) shifted to  $1,630\text{ cm}^{-1}$  (120 h) with time.

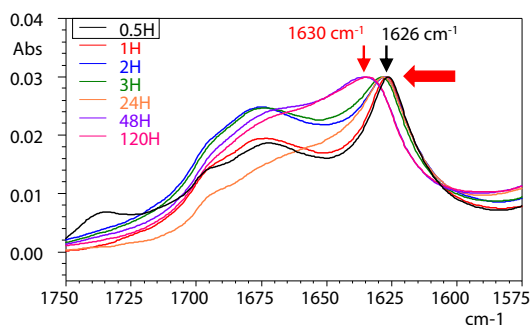


Fig. 2 Amide I Band in Infrared Spectrum

Fig. 3 shows the second derivative spectrum of amyloid- $\beta$ . The second derivative spectrum revealed that the intensities of the peaks at 1,696  $\text{cm}^{-1}$  and 1,626  $\text{cm}^{-1}$  decrease and the peak at 1,626  $\text{cm}^{-1}$  shifts to 1,630  $\text{cm}^{-1}$ . The peaks at 1,696  $\text{cm}^{-1}$  and 1,626  $\text{cm}^{-1}$  are a distinctive feature of antiparallel  $\beta$  sheets, whereas the peak at 1,630  $\text{cm}^{-1}$  is caused by parallel  $\beta$  sheets<sup>(5)</sup>. Fig. 4 shows the  $\beta$  sheet structure.

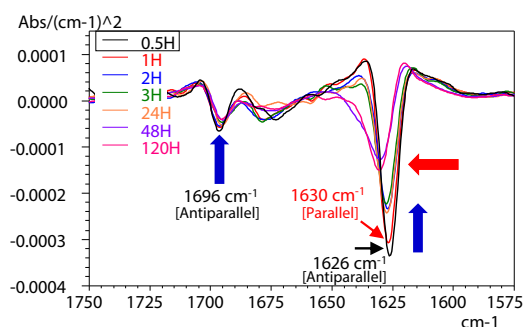


Fig. 3 Second Derivative Spectrum

Next, the secondary structures were identified by curve fitting of the amide I band. Fig. 5 shows the infrared spectra after 0.5 h and 120 h and the results of curve fitting. The peaks in the ranges of 1,700  $\text{cm}^{-1}$  to 1,690  $\text{cm}^{-1}$  (high wavenumber region) and 1,645  $\text{cm}^{-1}$  to 1,615  $\text{cm}^{-1}$  (low wavenumber region) were assigned to the  $\beta$  sheet<sup>(3)</sup>. Table 2 shows the sums of the peak areas and the ratios of the high and low wavenumber regions of the  $\beta$  sheets. The ratio after 0.5 h was 0.2836, suggesting a structure with a large fraction of antiparallel  $\beta$  sheets. After 120 h, the ratio decreased to 0.1860, clarifying the fact that conversion from the antiparallel  $\beta$  sheet structure to the parallel  $\beta$  sheet structure occurs over time, and the number of amyloid fibrils caused by formation of parallel  $\beta$  sheets also increases. This is the same result as the second derivative spectrum described above.

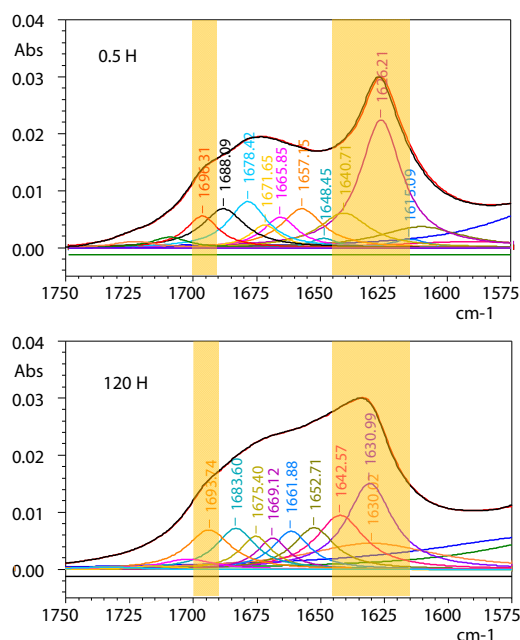


Fig. 5 Infrared Spectra and Results of Curve Fitting

Table 2 Sum of Peak Areas and Ratios of  $\beta$  Sheets

		0.5 h	120 h
Sum of peak areas	High wavenumber: 1,700 $\text{cm}^{-1}$ - 1,690 $\text{cm}^{-1}$	0.2371	0.2115
	Lower wavenumber: 1,645 $\text{cm}^{-1}$ - 1,615 $\text{cm}^{-1}$	0.8359	1.1372
Ratio (high wavenumber/low wavenumber)		0.2836	0.1860

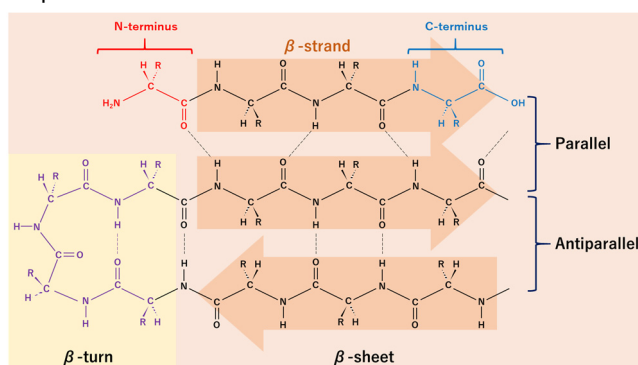


Fig. 4 Structure of  $\beta$  Sheet

## Conclusion

Amyloid- $\beta$  aggregation was evaluated by using FTIR. The results of an analysis of the amide I bands in the infrared spectrum and second derivative spectrum suggested that a time-dependent change (conversion from antiparallel  $\beta$  sheet structure to parallel  $\beta$  sheet structure) occurs in the secondary structure accompanying aggregation of amyloid- $\beta$ .

IRTracer is a trademark of Shimadzu Corporation in Japan and/or other countries.  
MicromATR is a trademark of Cziitek, LLC.

## <References>

- (1) Sean D. Moran and Martin T. Zanni, J. Phys. Chem. Lett. 2014, 5, 1984-1993
- (2) Mitsuo Tasumi, Infrared Spectroscopy – Fundamentals and Recent Techniques, ST Japan INC.
- (3) Jilie KONG, Shaoning YU. Fourier Transform Infrared Spectroscopic Analysis of Protein Secondary Structures. Acta Biochim Biophys Sin 2007, 39(8): 549–559
- (4) Youcef Fezoui, Amyloid: Int. J. Chin. Invest. 2000, 7, 166-178
- (5) Rabia Sarroukh, Erik Goormaghtigh, Jean-Marie Ruyschaert, Vincent Raussens, Biochimica et Biophysica Acta 1828 (2013) 2328–2338
- (6) JENNIFER KOVACS-NOLAN, J. Agric. Food Chem. 2005, 53, 8421-8431

First Edition: Jun. 2020



For Research Use Only. Not for use in diagnostic procedures.

This publication may contain references to products that are not available in your country. Please contact us to check the availability of these products in your country.

The content of this publication shall not be reproduced, altered or sold for any commercial purpose without the written approval of Shimadzu. Shimadzu disclaims any proprietary interest in trademarks and trade names used in this publication other than its own. See <http://www.shimadzu.com/about/trademarks/index.html> for details.

The information contained herein is provided to you "as is" without warranty of any kind including without limitation warranties as to its accuracy or completeness. Shimadzu does not assume any responsibility or liability for any damage, whether direct or indirect, relating to the use of this publication. This publication is based upon the information available to Shimadzu on or before the date of publication, and subject to change without notice.

Shimadzu Corporation

[www.shimadzu.com/an/](http://www.shimadzu.com/an/)